

Observing Dark Energy Dynamics with Supernova, Microwave Background and Galaxy Clustering

Jun-Qing Xia¹, Gong-Bo Zhao¹, Bo Feng², Hong Li¹ and Xinmin Zhang¹

¹*Institute of High Energy Physics, Chinese Academy of Science,*

P.O. Box 918-4, Beijing 100049, P. R. China and

²*Research Center for the Early Universe(RESCEU),*

Graduate School of Science, The University of Tokyo, Tokyo 113-0033, Japan

Observing dark energy dynamics is the most important aspect of the current dark energy research. In this paper we perform a global analysis of the constraints on the property of dark energy from the current astronomical observations. We pay particular attention to the effects of dark energy perturbations. Using the data from SNIa (157 "gold" sample), WMAP and SDSS we find that the best fitting dark energy model is given by the dynamical model with the equation of state across -1. Nevertheless the standard Λ CDM models are still a very good fit to the current data and evidence for dynamics is currently not very strong. We also consider the constraints with the recent released SNIa data from SNLS.

I. INTRODUCTION

In 1998 the analysis of the redshift-distance relation of Type Ia supernova (SNIa) has established that our universe is currently accelerating [1, 2]. Recent observations of SNIa have confirmed the accelerated expansion at high confidence level[3, 4, 5]. The nature of dark energy(DE), the mysterious power to drive the expansion, is among the biggest problems in modern physics and has been studied widely. A cosmological constant, the simplest candidate of DE where the equation of state (EOS) w remains -1, suffers from the well-known fine-tuning and coincidence problems[6, 7]. Alternatively, dynamical dark energy models with the rolling scalar fields have been proposed, such as quintessence[8, 9], the ghost field of phantom[10] and the model of k-essence which has non-canonical kinetic term[11, 12].

Given that currently we know very little on the theoretical aspects of dark energy, the cosmological observations play a crucial role in our understanding of dark energy. The model of phantom has been proposed in history due to the mild preference for a constant EOS smaller than -1 by the observations[10]. Although in this scenario dark energy violates the weak energy condition(WEC) and leads to the problem of quantum instabilities[13], it remains possible in the description of the nature of dark energy[14].

An intriguing aspect in the study of dark energy is that the recent SNIa observations from the HST/GOODS program[4], combined together with the previous supernova data, somewhat favor the dynamical dark energy model with an equation of state getting across -1 during the evolution of the universe[15, 16, 17, 18]. Although the conventional scalar dark energy models also show dynamical behaviors with redshift, due to the instabilities of perturbations they cannot preserve the required behavior of crossing the cosmological constant boundary[19, 20, 21]. The required model of dark energy has been called as quintom[18] in the sense that its behavior resemble the combined behavior of quintessence

and phantom. However, the quintom models can be very different from the quintessence or phantom in the determination of the evolution and fate of the universe[22]. There are a lot of interests in the literature recently in the building of quintom-like models. With minimally coupled to gravity a simple realization of quintom scenario is a model with the double fields of quintessence and phantom[18, 23, 24, 25, 26, 27, 28]. In such cases quintom would typically encounter the problem of quantum instability inherited in the phantom component. However in the case of the single field scalar model of quintom, Ref.[30] added a high derivative term to the kinetic energy and its energy-momentum tensor is equivalent to the two-field quintom model. Such a model with a high derivative term is possibly without quantum instabilities and as indicated by the SNIa observations, we are living with the ghosts [29]¹. Perturbations of the quintom-like models have been studied extensively in Ref.[20].

Observing the dark energy dynamics is currently the most important aspect of the dark energy study. Besides the SNIa data, a thorough investigation demands a fully consistent analysis of Cosmic Microwave Background(CMB), large scale structure(LSS) and with multi-parameter freedoms. The aim of current paper is to study the observational implications on dark energy in the consistent way. We extend our previous work of Ref.[20] and study the full observational constraints on dynamical dark energy. In particular we pay great attention to the effects of dark energy perturbations when the equation of state gets across -1. Our paper is structured as follows: in Section II we describe the method and the data; in Section III we present our results on the determination of cosmological parameters with the first year Wilkinson Microwave Anisotropy Probe (WMAP) [32], SNIa [4, 33] and Sloan Digital Sky Survey (SDSS) [34] data by global fittings using the Markov chain Monte

¹ For another interesting single field quintom model building see [31].

Carlo (MCMC) techniques [35, 36, 37]; finally we present our conclusions in Section IV.

II. METHOD AND DATA

In this section we firstly present the general formula of the dark energy perturbations in the full parameter space of w especially when it crosses over the cosmological constant boundary. In our MCMC fittings to WMAP, SNIa and SDSS, we adopt a specific parametrization of the equation of state.

Despite our ignorance of the nature of dark energy, it is natural to consider the DE fluctuation whether DE is regarded as scalar field or fluid. In the extant cases like the two-field-quintom model as well as the single field case with a high derivative term [20], the perturbation of DE is shown to be continuous when the EOS gets across -1. For the conventional parameterized equation of state one can easily reconstruct the potential of the scalar dark energy if the EOS does not get across -1. Resembling the multi-field model of quintom or quintom with high derivative terms, the potential of the quintom dark energy can be directly reconstructed from the parameterized EOS on either side of the cosmological constant boundary². In this paper we give a self-consistent method to handle the perturbation in all the allowed range of EOS especially for the region where EOS evolves close to and crosses -1.

For the parametrization of the EOS which gets across -1, firstly we introduce a small positive constant ϵ to divide the full range of the allowed value of the EOS w into three parts: 1) $w > -1 + \epsilon$; 2) $-1 + \epsilon \geq w \geq -1 - \epsilon$; and 3) $w < -1 - \epsilon$. Working in the conformal Newtonian gauge, one can describe the perturbations of dark energy as follows [38]:

$$\dot{\delta} = -(1+w)(\theta - 3\dot{\Phi}) - 3\mathcal{H}(c_s^2 - w)\delta \quad , \quad (1)$$

$$\dot{\theta} = -\mathcal{H}(1-3w)\theta - \frac{\dot{w}}{1+w}\theta + k^2\left(\frac{c_s^2\delta}{1+w} + \Psi\right) \quad . \quad (2)$$

Neglecting the entropy perturbation contributions, for the regions 1) and 3) the EOS is always greater than -1 and less than -1 respectively and perturbation is well defined by solving Eqs.(1,2). For the case 2), the perturbation of energy density δ and divergence of velocity, θ , and the derivatives of δ and θ are finite and continuous for the realistic quintom dark energy models. However for the perturbations of the parametrizations there is clearly

a divergence. In our study for such a regime, we match the perturbation in region 2) to the regions 1) and 3) at the boundary and set[20]

$$\dot{\delta} = 0 \quad , \quad \dot{\theta} = 0. \quad (3)$$

In our numerical calculations we've limited the range to be $|\Delta w = \epsilon| < 10^{-5}$ and we find our method is a very good approximation to the multi-field quintom, with the accuracy being greater than 99.999%.

In the study of this paper the parameterized EOS of dark energy is taken by[39]

$$w(z) = w_0 + w_1 \frac{z}{1+z}. \quad (4)$$

The method we adopt is based on the publicly available Markov Chain Monte Carlo package `cosmomc`[40, 41], which has been modified to allow for the inclusion of dark energy perturbations with EOS getting across -1[20]. We sample the following 8 dimensional set of cosmological parameters:

$$\mathbf{p} \equiv (\omega_b, \omega_c, \Theta_S, \tau, w_0, w_1, n_s, \log[10^{10} A_s]) \quad (5)$$

where $\omega_b = \Omega_b h^2$ and $\omega_c = \Omega_c h^2$ are the physical baryon and cold dark matter densities relative to critical density, Θ_S is the ratio (multiplied by 100) of the sound horizon and angular diameter distance, τ is the optical depth, A_s is defined as the amplitude of initial power spectrum and n_s measures the spectral index. Basing on the Bayesian analysis, we vary the above 8 parameters fitting to the observational data with the MCMC method. Throughout, we assume a flat universe and take the weak priors as: $\tau < 0.8$, $0.5 < n_s < 1.5$, $-3 < w_0 < 3$, $-5 < w_1 < 5$, a cosmic age tophat prior as $10 \text{ Gyr} < t_0 < 20 \text{ Gyr}$. Furthermore, we make use of the HST measurement of the Hubble parameter $H_0 = 100h \text{ km s}^{-1} \text{ Mpc}^{-1}$ [42] by multiplying the likelihood by a Gaussian likelihood function centered around $h = 0.72$ and with a standard deviation $\sigma = 0.08$. We impose a weak Gaussian prior on the baryon and density $\Omega_b h^2 = 0.022 \pm 0.002$ (1 σ) from Big Bang nucleosynthesis[43].

In our calculations we have taken the total likelihood to be the products of the separate likelihoods of CMB, SNIa and LSS. Alternatively defining $\chi^2 = -2 \log \mathcal{L}$, we get

$$\chi_{total}^2 = \chi_{CMB}^2 + \chi_{SNIa}^2 + \chi_{LSS}^2 \quad . \quad (6)$$

In the computation of CMB we have included the first-year temperature and polarization data [32, 44] with the routine for computing the likelihood supplied by the WMAP team [45]. In the computation of nonlinear evolution of the matter power spectra we have used the code of HALOFIT [46] and fitted to the 3D power spectrum of galaxies from the SDSS[34] using the code developed in Ref. [47]. In the calculation of the likelihood from SNIa we have marginalized over the nuisance parameter. For the main results of the current paper the supernova data

² Although the multi-field dark energy models are more challenging on theoretical aspects of naturalness, given that we know very little on the nature of dark energy, the energy momentum of such models can be identified with single field scalar dark energy with high derivative kinetic terms[30]. Our phenomenological formula of perturbations on DE corresponds to such models of multi-field (quintom) with a negligible difference around the crossing point of -1[20].

we use are the "gold" set of 157 SNIa published by Riess *et al* in [4]. In addition, we also consider the constraints from the distance measurements of the 71 high redshift type Ia supernova discovered during the first year of the 5-year Supernova Legacy Survey (SNLS)[33].

III. RESULTS

In this section we present our results, particularly focusing on the effects of the dark energy perturbation. We start with the descriptions on the background parameters, then present the constraints on dark energy parameters. At last we give our constraints on dark energy from the recent observational data of SNLS.

In Table 1 we list the mean 1σ constraints on the parameters with and without DE perturbations. We find that almost all the cosmological parameters are well determined in our both cases. However the reionization depth seems to be an exception where a vanishing τ cannot be ruled out. We notice the determination on τ is prior dependent. For example the WMAP collaboration have taken a prior like $\tau < 0.3$ [45, 48, 49], which leads to a relatively stringent constraint on τ by the observations and a nonzero τ is particularly favored by the high power of temperature-polarization cross correlation on the largest scales[50]. However when the strong prior on τ is dropped one will in general get a less stringent bound from the full observational constraints, as also shown in Ref. [47]. The prior on τ is somewhat crucial for our parameter estimation since its effects on CMB can be compensated with the tilt of the primordial scalar as well as the tensor spectrum. As we will show below it will also be correlated with the dark energy parameters due to the Integrated Sachs-Wolfe(ISW) effects.

In Fig.1 also we delineate the corresponding posterior one dimensional marginalized distributions of the cosmological parameters from the combined observations of WMAP, SDSS and SNIa. The dotted vertical lines shows the quantity of every parameter with (red) and without (blue) DE perturbation giving the maximum likelihood. Due to the fact that the peaks in the likelihood are different from the corresponding expectation values, the dashed lines in Fig.1 do not lie at the center of the projected likelihoods. A vanishing τ cannot be excluded by the full combined observations at high confidence level. For the order of parameters listed in (5) the best fit values constrained by the full dataset (WMAP + SNIa + SDSS) is $\mathbf{p}=(0.023,0.12,1.04,0.16,-1.30,1.25,0.995,3.23)$. And for comparison the resulting parameters when switching off dark energy perturbations are given by $\mathbf{p}=(0.023,0.12,1.05,0.14,-1.15,0.63,0.962,3.14)$. Comparing with the bottom of Table 1, although the minimum χ^2 values have not been affected significantly (up to 1) by dark energy perturbations, all the best fit parameters have been changed. Moreover, the allowed parameter space has been changed a lot and the constraints on the background parameters have been less stringent

when including the dark energy perturbations. This can also be clearly seen from the two dimensional contour plots on the background parameters in Fig.2. The reason is not difficult to explain. The ISW effects of the dynamical dark energy boosts the large scale power spectrum of CMB[20]. For a constant equation of state Ref. [51] has shown that when the perturbations of dark energy have been neglected incorrectly, a suppressed ISW will be resulted for quintessence-like dark energy and on the contrary, an enhanced ISW is led to by phantom-like dark energy. In this sense if we neglect dark energy contributions, there will be less degeneracy in the determination of dark energy as well as the relative cosmological parameters. However, dark energy perturbations are anti-correlated with the source of matter perturbations and this will lead to a compensation on the ISW effects, which result in a large parameter degeneracy[51]. In fact as we have shown that crossing over the cosmological constant boundary would not lead to distinctive effects[20], hence the effects of our smooth parametrization of EOS on CMB can also be somewhat identified with a constant effective equation of state[52]

$$w_{eff} \equiv \frac{\int da \Omega(a) w(a)}{\int da \Omega(a)}, \quad (7)$$

however the SNIa and LSS observations will break such a degeneracy. Thus for the realistic cases of including dark energy perturbations, the correlations between the dark energy and the background parameters as well as the auto correlations of the background cosmological parameters have been enlarged, as can be seen from Fig.2.

The contribution of dark energy perturbation affect significantly the distribution of w_0 and w_1 , which can also be seen from Fig.3 on the constrains in the (w_0, w_1) plane. For the parameters (w_0, w_1) the inclusion of the dark energy perturbation change its best fit values from $(-1.15, 0.63)$ to $(-1.30, 1.25)$. In Fig.3, from outside in, the contours shrink with adding 157 SNIa data provided by Riess *et al* and SDSS information. Dark energy perturbation introduces more degeneracy between w_0 and w_1 thus enlarges the contours significantly. For the discussion on dynamical dark energy we have separated the space of $w_0 - w_1$ into four areas by the lines of $w_0 = -1$ and $w_0 + w_1 = -1$. The areas will then represent the quintessence where the EOS is always no less than -1 (the area with $w > 1$ can be reached by quintessence with a negative potential[53]), Quintom A where w is phantom-like today but quintessence-like in the past, phantom where the EOS is always no larger than -1 and Quintom B where dark energy has $w > -1$ today but $w < -1$ at higher redshifts. From the figure we can see that dynamical dark energy with the four types are all allowed by the current observations and Quintom A seems to cover the largest area in the 2-dimensional contours with all the data we used.

As shown in Fig.3 that w_0 and w_1 are in strong correlations. The constraints on $w(z)$ are perhaps relatively model independent, as suggested by Ref.[54].

TABLE 1. Mean 1σ constrains on cosmological parameters using different combination of WMAP, SNIa and SDSS information with/without DE perturbation. For the weakly constrained parameters we quote the 95% upper limit instead.

	With DE Perturbation			Without DE Perturbation		
	WMAP	WMAP+SN	WMAP+SN+SDSS	WMAP	WMAP+SN	WMAP+SN+SDSS
$\Omega_b h^2$	$0.0232^{+0.0010}_{-0.0011}$	$0.0234^{+0.0010}_{-0.0011}$	0.0232 ± 0.0010	0.0235 ± 0.0013	0.0232 ± 0.0011	0.0230 ± 0.0009
$\Omega_c h^2$	0.124 ± 0.016	0.128 ± 0.018	0.123 ± 0.010	0.111 ± 0.020	0.119 ± 0.018	0.122 ± 0.010
Θ_s	1.046 ± 0.006	1.047 ± 0.006	1.046 ± 0.005	1.046 ± 0.006	1.046 ± 0.006	1.046 ± 0.005
τ	$< 0.256(95\%)$	$< 0.264(95\%)$	$< 0.256(95\%)$	$< 0.399(95\%)$	$< 0.324(95\%)$	$< 0.246(95\%)$
w_0	$-0.732^{+0.623}_{-0.613}$	$-1.172^{+0.231}_{-0.226}$	$-1.167^{+0.191}_{-0.190}$	$-0.617^{+0.193}_{-0.190}$	$-1.080^{+0.105}_{-0.087}$	$-1.098^{+0.078}_{-0.080}$
w_1	$< 1.59(95\%)$	$0.361^{+0.842}_{-0.883}$	$0.597^{+0.657}_{-0.713}$	$< 0.832(95\%)$	$0.359^{+0.287}_{-0.179}$	$0.416^{+0.293}_{-0.153}$
n_s	$0.977^{+0.029}_{-0.030}$	$0.986^{+0.030}_{-0.031}$	0.982 ± 0.030	$0.995^{+0.045}_{-0.041}$	$0.981^{+0.032}_{-0.033}$	$0.970^{+0.024}_{-0.025}$
$\log[10^{10} A_s]$	3.181 ± 0.134	3.207 ± 0.132	$3.180^{+0.125}_{-0.123}$	$3.245^{+0.202}_{-0.183}$	$3.206^{+0.153}_{-0.150}$	$3.157^{+0.118}_{-0.119}$
Ω_Λ	$0.703^{+0.073}_{-0.072}$	0.678 ± 0.045	$0.681^{+0.031}_{-0.030}$	0.681 ± 0.086	0.697 ± 0.048	0.686 ± 0.031
Age/GYr	13.45 ± 0.27	$13.57^{+0.30}_{-0.29}$	13.67 ± 0.24	13.60 ± 0.30	13.62 ± 0.29	13.67 ± 0.23
Ω_m	$0.297^{+0.072}_{-0.073}$	0.322 ± 0.045	$0.319^{+0.030}_{-0.031}$	0.319 ± 0.086	0.303 ± 0.048	0.314 ± 0.031
σ_8	$0.927^{+0.152}_{-0.154}$	$0.913^{+0.148}_{-0.150}$	$0.854^{+0.096}_{-0.097}$	0.818 ± 0.120	$0.890^{+0.117}_{-0.118}$	$0.882^{+0.073}_{-0.072}$
z_{re}	$14.35^{+4.71}_{-4.68}$	$14.72^{+4.90}_{-4.77}$	$14.41^{+4.97}_{-4.83}$	$17.17^{+6.94}_{-6.27}$	$15.49^{+5.69}_{-5.38}$	$13.73^{+4.78}_{-4.72}$
H_0	$71.71^{+7.95}_{-8.02}$	$68.66^{+2.44}_{-2.45}$	$67.90^{+2.48}_{-2.46}$	$66.04^{+6.41}_{-6.47}$	$68.89^{+2.52}_{-2.61}$	$68.07^{+2.35}_{-2.33}$
$\chi^2/d.o.f$	1429.1/1342	1610.4/1499	1633.2/1518	1428.4/1342	1610.6/1499	1634.1/1518

Following[55] we obtain the constraints on $w(z)$ by computing the median and $1, 2\sigma$ intervals at any redshift. In Fig.4 we plot the behavior of the dark energy EOS as a function of redshift z , we find that at redshift $z = 0.3$ the constraint on the EOS is relatively the most stringent. One can see that the perturbation reinforces the trend of DE to cross -1 at $z \sim 0.3$. However due to the limitation of the observational data, the quintom scenario is only favored at 1σ by the full dataset of WMAP, SDSS and SNIa. We find the value at $z = 0.3$ is restricted at

$$w(z = 0.3) = -1.002^{+0.044+0.180}_{-0.079-0.159} \quad (8)$$

for the case without dark energy perturbations and

$$w(z = 0.3) = -1.029^{+0.108+0.230}_{-0.098-0.288} \quad (9)$$

when including dark energy perturbations. Correspondingly at redshift $z = 1$ the constraints turn out to be

$$w(z = 1) = -0.890^{+0.180+0.193}_{-0.159-0.301} \quad (10)$$

without perturbations and

$$w(z = 1) = -0.868^{+0.215+0.520}_{-0.204-0.815} \quad (11)$$

when including dark energy perturbations. One should bear in mind that such a constraint is not really model independent, as shown in Refs. [56, 57].

Recently the authors of Ref.[33] made the distance measurements to 71 high redshift type Ia supernovae discovered during the first year of the 5-year Supernova Legacy Survey (SNLS). SNLS will hopefully discover around 700 type Ia supernovae, which is an intriguing ongoing project. Following Ref.[33] we combine

the "new 71 high redshift SNIa data \oplus the 44 nearby SNIa", together with WMAP and SDSS. We plot the constrains on the dark energy parameters in Fig.5. We find the current data of SNLS are very weak in the determination of dark energy parameters. Although our best fit values are given with a quintom like dark energy: $(w_0, w_1) = (-1.47, 1.44)$, a cosmological constant fits well with SNLS in the 1σ region.³

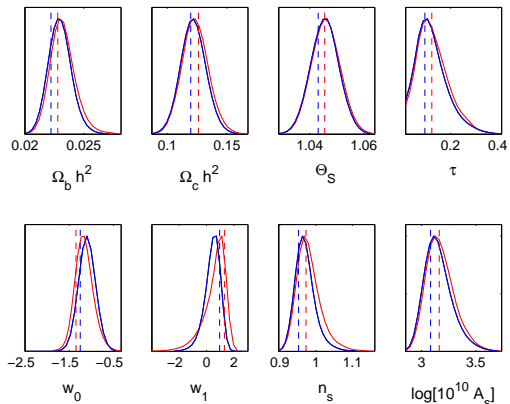


FIG. 1: 1-D constrains on individual parameters using WMAP+157 "gold" SNIa+SDSS with our 8-parameter parametrization discussed in the text. Solid curves illustrate the marginalized distribution of each parameter with(red) and without(blue) DE perturbation. Dotted vertical lines shows the quantity of every parameter with (red) and without (blue) DE perturbation giving the maximum likelihood.

³ Ref. [58] made some study on SNLS implications of dynamical dark energy using SNIa data only.

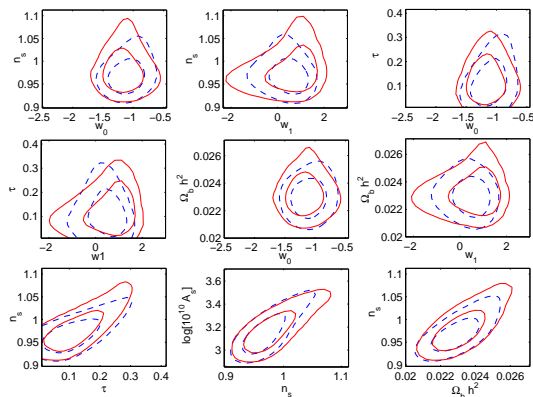


FIG. 2: Sampled 2-D contours of the background parameters and also the contours among dark energy and the background parameters. Here we use the same parametrization and data sets as FIG.2, red solid and blue dashed lines are for perturbed and unperturbed DE respectively.

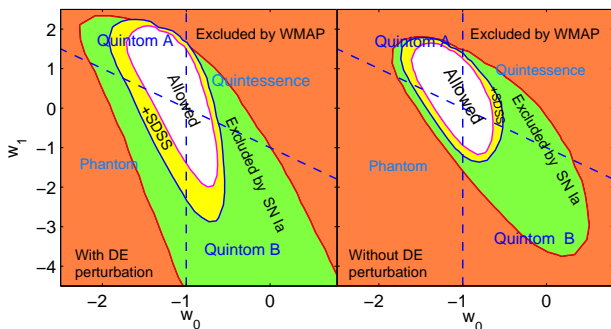


FIG. 3: 95% constrains in the (w_0, w_1) plane with and without dark energy perturbation from left to right. Shaded dark orange region is excluded by WMAP only for our 8-parameter estimation. The dashed lines stand for $w_0 = -1$ and $w_0 + w_1 = -1$, see the text for details.

IV. DISCUSSION AND CONCLUSION

In this paper we have performed an analysis of global fitting on the EOS of dark energy from the current data of SNIa, WMAP and SDSS. Dark energy perturbation leaves imprints on CMB through ISW effects and changes the matter power spectrum by modifying the linear growth factor as well as the transfer function. Our results show that when we include the perturbations of dark energy, the current observations allow for a large variation in the EOS of dark energy with respect to redshift⁴. A dynamical dark energy with the EOS getting

⁴ Ref. [59] studied the perturbations of dynamical dark energy only for the regime where $w > -1$ and Ref. [60] considered both the cases for $w > -1$ and $w < -1$, but did not include the per-

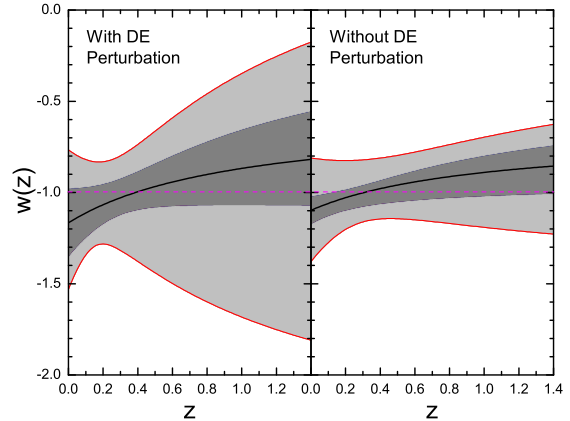


FIG. 4: Constrains on $w(z)$ using WMAP + 157 "gold" SNIa data + SDSS with/without DE perturbation. Median(central line), 68%(inner, dark grey) and 95%(outer, light grey) intervals of $w(z)$ using 2 parameter expansion of the EOS in (4).

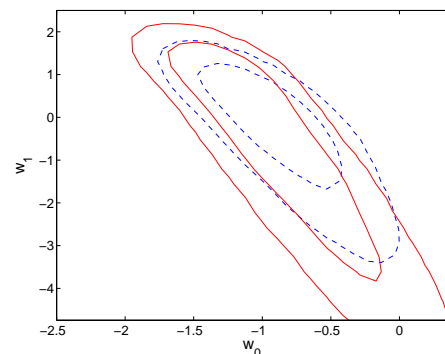


FIG. 5: Two dimensional constraints on the parameters of dynamical dark energy from the combined constraints of SNLS, WMAP and SDSS. The solid and dotted lines are the constraints with and without dark energy perturbations, respectively.

across -1 is favored at 1σ with the combined constraints from WMAP, SDSS and the "gold" dataset of SNIa by Riess *et al.* When we use the recently released SNLS data and the nearby data of type Ia supernova instead, the parameter space is enlarged and a cosmological constant is well within 1σ , although a quintom dynamical dark energy is still mildly favored.

In our all results, the perturbation of dark energy plays a significant role in the determination of cosmological parameters. Neglecting the contributions of dark energy perturbation will lead to biased results which are more

turbations for quintom like dark energy; previous global analysis like Ref. [54, 61] did not consider dark energy perturbations.

stringent than the real cases. In the next decade, there will be many ongoing projects in the precise determination of cosmological parameters. We can hopefully detect the signatures of dynamical dark energy like quintom through global fittings to the observations, where it is crucial for us to include the contributions of dark energy perturbations.

Acknowledgements: Our MCMC chains were fin-

ished in the Shuguang 4000A system of the Shanghai Supercomputer Center(SSC). This work is supported in part by National Natural Science Foundation of China under Grant Nos. 90303004, 10533010 and 19925523 and by Ministry of Science and Technology of China under Grant No. NKBRF G19990754. We thank Mingzhe Li for helpful discussions and Hiranya Peiris for comments on the manuscript.

-
- [1] A.G. Riess *et al.* (Supernova Search Team Collaboration), *Astron. J.* **116**, 1009 (1998).
- [2] S. Perlmutter *et al.* (Supernova Cosmology Project Collaboration), *Astrophys. J.* **517**, 565 (1999).
- [3] J. L. Tonry *et al.* (Supernova Search Team Collaboration), *Astrophys. J.* **594**, 1 (2003).
- [4] A. G. Riess *et al.* (Supernova Search Team Collaboration), *Astrophys. J.* **607**, 665 (2004).
- [5] A. Clocchiatti *et al.* (the High Z SN Search Collaboration), *astro-ph/0510155*.
- [6] S. Weinberg, *Rev. Mod. Phys.* **61**, 1 (1989).
- [7] I. Zlatev, L.-M. Wang, and P. J. Steinhardt, *Phys. Rev. Lett.* **82**, 896 (1999).
- [8] B. Ratra and P. J. E. Peebles, *Phys. Rev. D* **37**, 3406 (1988); P. J. E. Peebles and B. Ratra, *Astrophys. J.* **325**, L17 (1988).
- [9] C. Wetterich, *Nucl. Phys. B* **302**, 668 (1988); C. Wetterich, *Astron. Astrophys.* **301**, 321 (1995).
- [10] R. R. Caldwell, *Phys. Lett. B* **545**, 23 (2002).
- [11] T. Chiba, T. Okabe and M. Yamaguchi, *Phys. Rev. D* **62** (2000) 023511.
- [12] C. Armendariz-Picon, V. Mukhanov and P. J. Steinhardt, *Phys. Rev. Lett.* **85**, 4438 (2000); *Phys. Rev. D* **63**, 103510 (2001).
- [13] S. M. Carroll, M. Hoffman and M. Trodden, *Phys. Rev. D* **68**, 023509 (2003); J. M. Cline, S.-Y. Jeon and G. D. Moore, *Phys. Rev. D* **70**, 043543 (2004).
- [14] e. g. P. H. Frampton, *Phys. Lett. B* **555**, 139 (2003); V. Sahni and Y. Shtanov, *J. Cosmol. Astropart. Phys.* **0311**, 014 (2003); B. McInnes, *J. High Energy Phys.* **0208**, 029 (2002); V.K. Onemli and R.P. Woodard, *Class. Quant. Grav.* **19**, 4607 (2002); V. K. Onemli and R. P. Woodard, *Phys. Rev. D* **70**, 107301 (2004); I. Y. Aref'eva, A.S. Koshelev and S.Y. Vernov, *astro-ph/0412619*; I. Y. Aref'eva and L. V. Joukovskaya, *JHEP* **0510**, 087 (2005).
- [15] S. Nesseris and L. Perivolaropoulos, *Phys. Rev. D* **70**, 043531 (2004).
- [16] U. Alam, V. Sahni and A. A. Starobinsky, *J. Cosmol. Astropart. Phys.* **0406**, 008 (2004).
- [17] D. Huterer and A. Cooray, *Phys. Rev. D* **71**, 023506 (2005).
- [18] B. Feng, X. Wang, and X. Zhang, *Phys. Lett. B* **607**, 35, (2005).
- [19] A. Vikman, *Phys. Rev. D* **71**, 023515 (2005).
- [20] G. B. Zhao, J. Q. Xia, M. Li, B. Feng and X. Zhang, *astro-ph/0507482*.
- [21] L. R. Abramo and N. Pinto-Neto, *astro-ph/0511562*.
- [22] B. Feng, M. Li, Y. S. Piao and X. Zhang, *astro-ph/0407432*.
- [23] Z.-K. Guo, Y.-S. Piao, X. Zhang and Y.-Z. Zhang, *Lett. B* **608**, 177, (2005).
- [24] W. Hu, *Phys.Rev. D* **71** (2005) 047301.
- [25] X. Zhang, *hep-ph/0410292*.
- [26] R. R. Caldwell and M. Doran, *Phys. Rev. D* **72**, 043527 (2005).
- [27] X.-F. Zhang, H. Li, Y.-S. Piao, and X. Zhang, *astro-ph/0501652*.
- [28] For an interesting variation see H. Wei, R. G. Cai and D. F. Zeng, *Class. Quant. Grav.* **22**, 3189 (2005).
- [29] S. W. Hawking and T. Hertog, *Phys.Rev. D* **65**, 103515 (2002).
- [30] M. Li, B. Feng and X. Zhang, *hep-ph/0503268*.
- [31] C. G. Huang and H. Y. Guo, *astro-ph/0508171*.
- [32] C. L. Bennett *et al.* (WMAP Collaboration), *Astrophys. J. Suppl.* **148**, 1 (2003).
- [33] P. Astier *et al.*, *astro-ph/0510447*.
- [34] M. Tegmark *et al.* (SDSS Collaboration), *Astrophys. J.* **606**, 702 (2004).
- [35] D. Gamerman, *Markov Chain Monte Carlo: Stochastic simulation for Bayesian inference* (Chapman and Hall, 1997).
- [36] D. J. C. MacKay (2002), <http://www.inference.phy.cam.ac.uk/mackay/itprnn/book.html>.
- [37] R. M. Neil (1993), <ftp://ftp.cs.utoronto.ca/pub/~radford/review>.
- [38] C. -P. Ma and E. Berschinger, *Astrophys. J.* **455** 7, (1995).
- [39] M. Chevallier and D. Polarski, *Int. J. Mod. Phys. D* **10**, 213(2001); E. V. Linder, *Phys. Rev. Lett.* **90**, 091301 (2003).
- [40] A. Lewis and S. Bridle, *Phys. Rev. D* **66**, 103511 (2002).
- [41] Available from <http://cosmologist.info>.
- [42] W. L. Freedman *et al.*, *Astrophys. J.* **553**, 47 (2001).
- [43] S. Burles, K. M. Nollett and M. S. Turner, *Astrophys. J.* **552**, L1 (2001).
- [44] G. Hinshaw *et al.*, *Astrophys. J. Suppl.* **148**, 345 (2003).
- [45] L. Verde *et al.* (WMAP Collaboration), *Astrophys. J. Suppl.* **148**, 195 (2003).
- [46] R. E. Smith *et al.*, *Mon. Not. Roy. Astron. Soc.* **341**, 1311 (2003).
- [47] M. Tegmark *et al.* (SDSS Collaboration), *Phys. Rev. D* **69**, 103501 (2004).
- [48] D. N. Spergel *et al.* (WMAP Collaboration), *Astrophys. J. Suppl.* **148**, 175 (2003).
- [49] H. V. Peiris *et al.* (WMAP Collaboration), *Astrophys. J. Suppl.* **148**, 213 (2003).
- [50] A. Kogut *et al.* (WMAP Collaboration), *Astrophys. J. Suppl.* **148**, 161 (2003).
- [51] J. Weller and A. M. Lewis, *Mon. Not. Roy. Astron. Soc.* **346**, 987 (2003).
- [52] e.g. L. M. Wang, R. R. Caldwell, J. P. Ostriker and P. J. Steinhardt, *Astrophys. J.* **530**, 17 (2000).
- [53] See e.g. G. N. Felder, A. V. Frolov, L. Kofman and

- A. V. Linde, Phys. Rev. D **66** (2002) 023507.
- [54] U. Seljak *et al.*, Phys. Rev. D **71**, 103515 (2005).
- [55] D. Huterer and M. S. Turner, Phys. Rev. D **64**, 123527 (2001).
- [56] B. A. Bassett, P. S. Corasaniti and M. Kunz, Astrophys. J. **617**, L1 (2004).
- [57] J.-Q. Xia, B. Feng, and X. Zhang, Mod. Phys. Lett. A **20**, 2409 (2005).
- [58] S. Nesseris and L. Perivolaropoulos, astro-ph/0511040.
- [59] Ch. Yeche, A. Ealet, A. Refregier, C. Tao, A. Tilquin, J.-M. Virey and D. Yvon, astro-ph/0507170.
- [60] P. S. Corasaniti, M. Kunz, D. Parkinson, E. J. Copeland and B. A. Bassett, Phys. Rev. D **70**, 083006 (2004).
- [61] S. Hannestad and E. Mortsell, J. Cosmol. Astropart. Phys. **0409** 001 (2004); A. Upadhye, M. Ishak and P. J. Steinhardt, Phys. Rev. D **72**, 063501 (2005).